Applied Catalysis B: Environmental 160–161 (2014) 542–551

Contents lists available at ScienceDirect

Applied Catalysis B: Environmental

journal homepage: www.elsevier.com/locate/apcatb

A comparative study of the catalytic oxidation of HCHO and CO over $Mn_{0.75}Co_{2.25}O_4$ catalyst: The effect of moisture

Yu Wang[a,b], Xiaobing Zhu[b], Mark Crocker[c], Bingbing Chen[a,b], Chuan Shi[a,b,*]

[a] Key laboratory of Industrial Ecology and Environmental Engineering (MOE), Dalian University of Technology, Dalian, People's Republic of China
[b] Laboratory of Plasma Physical Chemistry, Dalian University of Technology, Dalian, People's Republic of China
[c] Center for Applied Energy Research, University of Kentucky, Lexington, KY 40511, USA

ARTICLE INFO

Article history:
Received 23 February 2014
Received in revised form 5 May 2014
Accepted 8 June 2014
Available online 13 June 2014

Keywords:
$Mn_{0.75}Co_{2.25}O_4$ catalyst
HCHO oxidation
CO oxidation
Water influence
Stability

ABSTRACT

The influence of moisture on the activity and stability of $Mn_{0.75}Co_{2.25}O_4$ catalyst for HCHO and CO oxidation was compared and investigated. Totally opposite effects of relative humidity (RH) on the reactions were observed: with increase of RH (0–90%), the activity for HCHO oxidation was enhanced, whereas the activity for CO oxidation was greatly decreased. However, in both cases the catalyst lifetime was prolonged in the presence of moisture (RH = 50%). Such modifications were directly evidenced by correlating in-situ DRIFTS data, TPO results and MS–IRAS studies, which clarified the effects of water on the activity and stability of $Mn_{0.75}Co_{2.25}O_4$ catalyst for HCHO and CO oxidation.

1. Introduction

The removal of air pollutants by low-temperature catalytic oxidation is gaining increasing importance as a technology that can meet the strict limits required by world-wide environmental regulations [1,2]. In general, low-temperature catalytic oxidation is known to be greatly influenced by moisture in the reactant gas, the presence of which is unavoidable in most applications. Interestingly, water can play different roles in the same reaction over different kinds of catalysts. As observed for low temperature CO oxidation, a moderate amount of water on the surface of precious metals such as Au, Pt, Ru, and Pd can promote the reaction [3–11]. On the other hand, it can act as a poison on the surface of metal oxides, such as Co_3O_4, CuO, and MnO_x [12–19]. However, in the case of HCHO oxidation the situation is less clear-cut; indeed, there is considerable debate over the exact role of water in HCHO oxidation. Addition of water to the reactant stream was found to increase HCHO conversion over Pt/Fe_2O_3, Au/CeO_2, MnO_x and $Ag–MnO_x–CeO_2$ catalysts [20–23]. Huang et al. [24] found water vapor is essential to HCHO oxidation. Hydroxyl radical (OH) from water vapor dissociation favors the adsorption and transfer of oxygen on the Pd/TiO_2 catalysts, which is very important during HCHO oxidation. However, a decrease in catalytic activity was also reported for Pd/Al_2O_3, $Fe_2O_3–MnO_2$, $CuO–MnO_2$, AgCu/HZ, $MnO_x–CeO_2$ and MnO_x catalysts [25–28]. Moreover, whereas HCHO is water soluble, CO is water insoluble, a fact which might be expected to influence the effect that water exerts in CO and HCHO catalytic oxidation. The apparently contrary properties H_2O in these reactions prompted us to compare the effect of moisture on catalyst activity and stability in low temperature CO and HCHO oxidation.

A $Mn_{0.75}Co_{2.25}O_4$ solid solution catalyst has been reported by our group to be a stable and active catalyst for HCHO oxidation [29], although no papers devoted to CO oxidation on $Mn_{0.75}Co_{2.25}O_4$ have been published to date. Therefore, in the present study a $Mn_{0.75}Co_{2.25}O_4$ solid solution catalyst was selected as the target catalyst, on which the effects of moisture on HCHO oxidation and CO oxidation were compared. Moisture was found to play a totally different role in the two reactions, showing positive effects for HCHO oxidation with respect to both catalyst activity and stability, while in CO oxidation negative and positive effects were observed with respect to catalyst activity and stability, respectively. By using in situ diffuse reflectance infrared Fourier transform spectroscopy (DRIFTS) and temperature-programmed oxidation reaction (TPO),

* Corresponding author at: Key laboratory of Industrial Ecology and Environmental Engineering (MOE), Dalian University of Technology, Dalian, People's Republic of China. Tel.: +86 411 84986083.
E-mail address: chuanshi@dlut.edu.cn (C. Shi).

http://dx.doi.org/10.1016/j.apcatb.2014.06.011
0926-3373/

the roles of H_2O in HCHO and CO catalytic oxidation were illuminated.

2. Experimental

2.1. Catalyst preparation

The $Mn_{0.75}Co_{2.25}O_4$ catalyst was prepared by a co-precipitation method as reported previously [28]. Typically, an aqueous solution of Na_2CO_3 was added dropwise to $Mn(NO_3)_2$ and $Co(NO_3)_2{\cdot}6H_2O$ (Mn/Co = 1/3, atomic ratio) under vigorous agitation to reach a pH value of 9.0. After an ageing period of 3 h, the solid was isolated by filtration, was washed, dried at 80 °C overnight, and calcined in air at 350 °C for 5 h.

2.2. Catalyst characterization

Infrared spectra were recorded on a DRIFT spectrometer (Bruker-Tensor-27, Germany) equipped with a mercury cadmium tellurium (MCT) detector. The DRIFT spectra were acquired at a resolution of 4 cm^{-1}. Typically, 128 scans were taken. The $Mn_{0.75}Co_{2.25}O_4$ sample was pretreated in a N_2 (99.99%) flow of 50 ml/min at 350 °C for 1 h and a background spectrum in N_2 flow was acquired at each measurement temperature.

TPO experiments were used to study the gas phase products during the interaction of surface intermediates with O_2. The sample was first pretreated in a N_2 stream (flow rate = 50 ml/min) at 350 °C for 1 hand then cooled to room temperature. Next, a gas stream was introduced containing dry or humid air (80 ppm HCHO/21%O_2/H_2O (RH = 0 or 50%)/N_2 balance) (flow rate = 100 ml/min) for 60 min to facilitate HCHO adsorption. The catalyst was purged with a dry simulated air stream at a flow rate of 100 ml/min at room temperature for 30 min before TPO. Finally, oxidation in a gas stream containing 21% O_2/N_2 balance (flow rate = 100 ml/min) was carried out from room temperature to 350 °C at a rate of 10 °C/min. The gas products were analyzed by an on-line CO_x analyzer (SICK-MAIHAK-S710, Germany).

An online mass spectrometer (MS, Omini-star, GSD-301) equipped with a fast-response inlet capillary/leak diaphragm system along with an infrared absorption spectrometer (IRAS, SICK-MAIHAK, S710) was used to analyze effluent gases. The concentration of H_2O was determined using $m/z = 18$, and those of CO and CO_2 in the gas phase were determined by IRAS.

2.3. Catalytic activity measurement

2.3.1. Catalyst evaluation

All the feed gases used in this work were of high-purity grade (99.99%). The gas flow rates were adjusted and controlled by mass flow controllers. Gaseous HCHO was generated by flowing N_2 over paraformaldehyde (99%, Aldrich) in a thermostated water bath (the concentration of HCHO was controlled by adjusting the flow rate of N_2 and the temperature of the water bath). Gaseous H_2O was introduced into the gas stream by passing N_2 through a bubbler in a water bath at room temperature. The water content of the gas, expressed as the relative humidity (RH) at 25 °C, was controlled by adjusting the flow rate of N_2, while keeping the total flow unchanged.

The reactant feed was: (i) a mixed gas stream of 80 ppm HCHO/21 vol.% O_2/N_2 (0–90% relative humidity (RH, 25 °C)) and (ii) a mixed gas stream of 500 ppm CO/21 vol.% O_2/N_2 (0–90% relative humidity (RH, 25 °C)). The HCHO or CO mixed gas stream was fed into a fixed-bed reactor and passed through the catalyst bed (150 mg, 40–60 mesh) at a flow rate of 100 ml/min (GHSV = 60,000 h^{-1}). The concentration of HCHO (0–100 ppm) was measured by converting it to CO_2 in a homemade HCHO-to-CO_2 converter(CuO–MnO_2/γ-Al_2O_3 catalyst) [21,23,29,30] at 400 °C and determining the amount of CO_2 formed using a CO_x analyzer. The concentration of CO (0–1000 ppm) was measured by the CO_x analyzer directly. The conversion of HCHO or CO to CO_2 was quantified on the basis of the carbon balance with an accuracy of >95%. Thus, HCHO or CO conversion was calculated as follows:

$$\text{HCHO conversion } (\%) = \frac{n_{CO_2}^{out}}{n_{HCHO}^{in}} \times 100\%,$$

$$\text{CO conversion } (\%) = \frac{n_{CO_2}^{out}}{n_{CO}^{in}} \times 100\%,$$

where $n_{CO_2}^{out}$ was the CO_2 concentration in the products, and n_{HCHO}^{in} and n_{CO}^{in} were the HCHO and CO concentrations in the feed gas.

2.3.2. The isothermal reaction

The intrinsic activity of the catalyst was based on the rate per unit of surface area or the TOFs ($\mu mol_{HCHO}/(s\,m^2{}_{cat})$ or $\mu mol_{CO}/(s\,m^2{}_{cat})$) value, which was defined as the ratio of the reaction rate to the active site density of catalysts. The reaction rate of HCHO and CO combustion was determined by an isothermal reaction at 20–60 °C in the kinetic regime; the influences of internal and external mass and heat transfer were all excluded (see Figs. 1S and 2S). The total flow rate was 100 ml/min, and the reaction gas composition was the same as for the reaction. The selection of 20–60 °C was made because the HCHO and CO conversion was low (<20%) and nearly constant over time. For a total flow rate of 100 ml/min, no external mass transport limitations were detected. The gas analyses were then used to calculate the reaction rate (v) and the specific reaction rate normalized by unit BET surface area (v^*) for HCHO and CO combustion using the equation

$$v = -\frac{dn}{mdt} = \frac{CO_2 \times Q_C}{m}[\text{mol/s g}_{cat}];$$

$$v* = \frac{v}{S} = \frac{CO_2 \times Q_C}{mS} \quad [\text{mol/s m}^2_{cat}]$$

where CO_2 is the measured molar fraction of these species in the gasphase, Q_C is the molar flow rate of gases through the reactor (mol/s), m is the mass of the catalyst (g), and S is the BET surface area of the catalyst (m^2/g).

Supposing that the reaction is a first-order reaction for HCHO and CO oxidation in the presence of excess oxygen [31–34], the obtained kinetic models are:

$$\ln v* = -\frac{E_a}{RT} - \ln k_0 + \ln C_{HCHO} \quad \text{and} \quad \ln v* = -\frac{E_a}{RT} - \ln k_0 + \ln C_{CO}$$

Let $y = \ln v^*$ and Let $x = 1000/T$, the Arrhenius plots can be given, as shown in Fig. 1B and Fig. 2B. As a result, parameters E_a can be estimated by the Levenberg–Marquardt method using the experiment data listed in Tables 2S and 3S.

3. Results

3.1. Moisture effects on catalyst activity and stability

The $Mn_{0.75}Co_{2.25}O_4$ catalyst was characterized in detail in our previous paper [29]. In summary, the sample possessed a specific surface area of 157 m^2/g, with an average crystal size of ca. 9 nm estimated from XRD and TEM measurements. The incorporation of manganese into Co_3O_4 to form a $Mn_xCo_{3-x}O_4$ solid solution was confirmed by the linear increase of the "d" value with increasing Mn content up to a Co/Mn ratio of 3/1. Such incorporation leads to enrichment of adsorbed surface oxygen species and better lower-temperature reducibility as evidenced by XPS and H_2-TPR results.

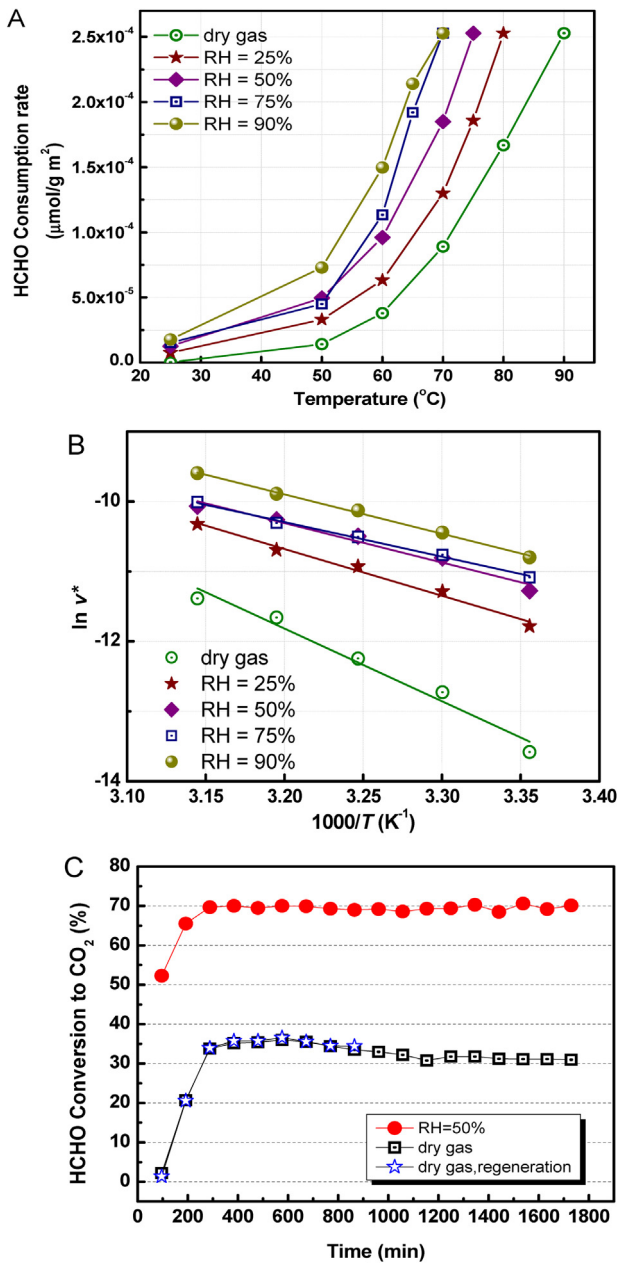

Fig. 1. (A) HCHO consumption rate as a function of reaction temperature over the $Mn_{0.75}Co_{2.25}O_4$ catalyst (80 ppm HCHO/21% O_2/H_2O (RH = 0–90%)/N_2 balance, GHSV = 60,000 h^{-1}). (B) Arrhenius plots for total oxidation of HCHO on the $Mn_{0.75}Co_{2.25}O_4$ catalyst. (C) Stability test performed using $Mn_{0.75}Co_{2.25}O_4$ catalyst (80 ppm HCHO/21% O_2/H_2O (RH = 0 or 50%)/N_2 balance, GHSV = 60,000 h^{-1}, reaction temperature = 70 °C).

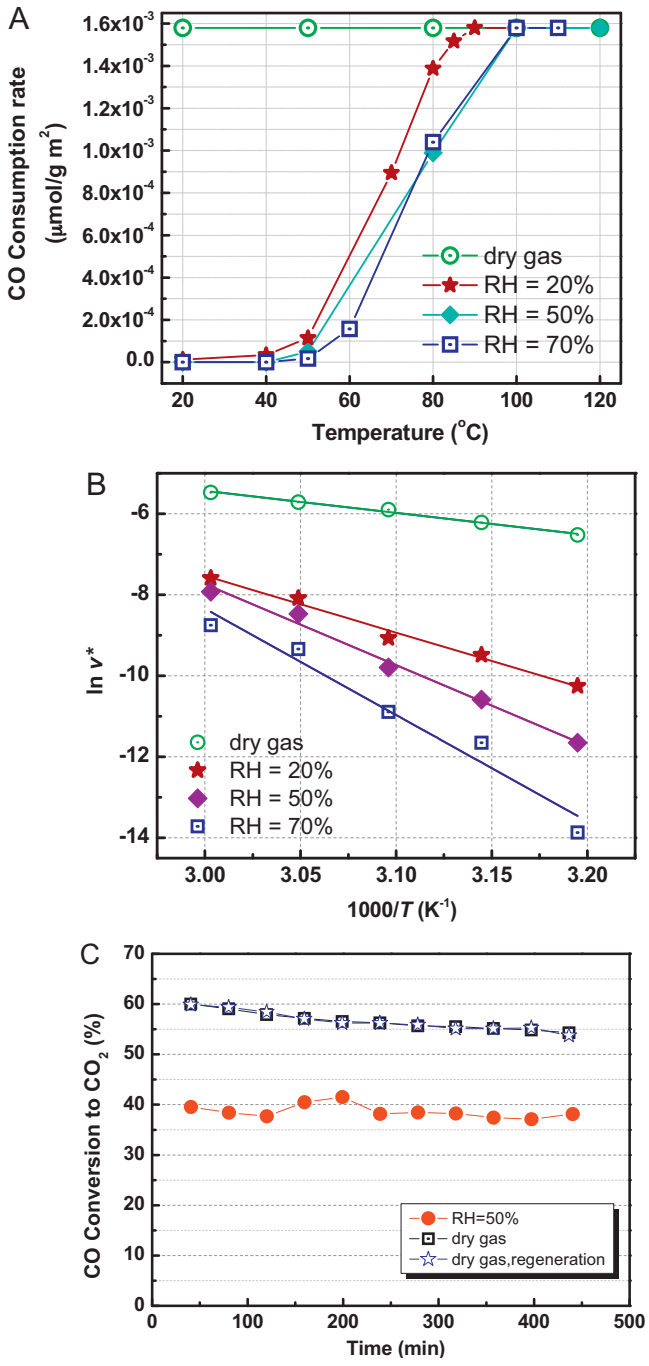

Fig. 2. (A) CO consumption rate as a function of reaction temperature over the $Mn_{0.75}Co_{2.25}O_4$ catalyst (500 ppm CO/20% O_2/H_2O (RH = 0–70%)/N_2 balance, GHSV = 60,000 h^{-1}). (B) Arrhenius plots for total oxidation of CO on the $Mn_{0.75}Co_{2.25}O_4$ catalyst. (C) Stability test performed using $Mn_{0.75}Co_{2.25}O_4$ catalyst (500 ppm CO/20% O_2/H_2O (RH = 0 or 50%)/N_2 balance, GHSV = 240,000 h^{-1}, reaction temperature = 90 °C).

Fig. 1 shows the HCHO consumption rate variation with reaction temperature over $Mn_{0.75}Co_{2.25}O_4$ catalyst at five relative humidity (RH) levels. It is clear that HCHO consumption rate was obviously enhanced with increase of react temperature. The highest rate was obtained at or above 70 °C, which is influenced by relative humidity. Notably, with increase of RH from 0 to 90%, HCHO consumption rate was obviously improved. The highest rate was obtained at 90 °C in dry gas, while it was decreased to 70 °C with RH increased to 75% and 90%. These results indicate that the presence of moisture in the feed has positive effect on HCHO oxidation over$Mn_{0.75}Co_{2.25}O_4$ catalyst within the tested RH range.

To further check for the moisture effects on HCHO oxidation, we carried out kinetics tests with both the humid and dry gas conditions over the $Mn_xCo_{3-x}O_4$ catalyst. Fig. 1B shows Arrhenius plots for the rates of HCHO oxidation at their conversion <20% (at which the reaction temperature range was 20–60 °C), respectively. As summarized in Table 1, the apparent activation energy (E_a) of the HCHO oxidation reaction was 86 kJ/mol of the dry gas condition, which was much higher than those (41–55 kJ/mol) of the humid gas conditions, with the RH increased to 75%, the $Mn_xCo_{3-x}O_4$ catalyst exhibiting the lowest E_a values (41 kJ/mol), thus providing further evidence that the rate per unit of surface area was increased by

Table 1
Activation energies (E_a) for the oxidation of HCHO and CO over the $Mn_{0.75}Co_{2.25}O_4$ catalyst.

HCHO oxidation		CO oxidation	
Conditions	E_a (kJ/mol)	Conditions	E_a (kJ/mol)
Dry gas	86	Dry gas	45
RH = 25%	55	RH = 20%	116
RH = 50%	47	RH = 50%	166
RH = 75%	41	RH = 70%	218
RH = 90%	46		

moisture within the tested range on the $Mn_{0.75}Co_{2.25}O_4$ catalyst, and indicating that the presence of moisture might provide another pathway with lower E_a, compared with that in dry gas.

Compared with transition metal oxide-based catalysts reviewed by Torres et al. [35] and summarized in Table 1S, it could be seen that the temperatures for complete HCHO oxidation overtransition metal oxide-based catalysts were often higher than 100 °C. Herein, the $Mn_{0.75}Co_{2.25}O_4$ exhibited one of the best catalytic performances among the transition metal oxide-based catalysts, showed a rate per unit of surface area of 2.04×10^{-5} $\mu mol_{HCHO}/(s\,m^2_{cat})$ at RH = 90% and 25 °C, which was higher than the reported transition metal oxide-based catalysts.

Fig. 1C shows the variations in HCHO conversion to CO_2 with time-on-stream (TOS) over the $Mn_{0.75}Co_{2.25}O_4$ catalyst in dry and humid (RH = 50%) air streams. It can be seen that the HCHO conversion to CO_2 in a dry air stream gradually decreased from 35% to 29%. In contrast, in a humid air stream (RH = 50%), HCHO conversion to CO_2 remained at 70% during the entire test.

Unlike the dramatic increase in activity observed in HCHO oxidation, the opposite effect was observed in CO oxidation, i.e., the presence of water decreased the CO consumption rate of $Mn_{0.75}Co_{2.25}O_4$, as shown in Fig. 2A. The highest CO consumption rate correspond to 100% CO conversion was obtained in dry air, even at RT. Comparatively the react rate was much lower in humid air, and there was no CO consumption observed at RT. With increase of react temperature, the CO consumption rate was accelerated, and reached its maximum at 85 °C with RH of 20%. While for RH of 50% and 70%, the highest CO consumption was obtained at 100 °C. The results clearly proved that the presence of moisture in feed gas depressed the activity of $Mn_{0.75}Co_{2.25}O_4$ catalyst for CO oxidation, which is contrast with HCHO oxidation.

Also, the kinetic tests were conducted to further check the moisture effect on CO oxidation. Fig. 2B shows Arrhenius plots for the rate of CO oxidation at the conversion <20% (at which the reaction temperature range was 40–60 °C), as summarized in Table 1, it is obvious that the activation energy of dry condition is the lowest (45 kJ/mol), which was much lower than those (116–218 kJ/mol) of the humid gas conditions, which suggested that the reaction was harder to activate in the presence of H_2O.

Fig. 2C shows the variation in CO conversion to CO_2 with TOS over the $Mn_{0.75}Co_{2.25}O_4$ catalyst in dry and humid (RH = 50%) air streams at 90 °C. In the presence of moisture, the CO conversion remained at ca. 40% for the duration of the test (450 min). In contrast, when a dry feed was used the catalyst slowly lost activity with time on stream, the CO conversion decreasing from 60% to ca. 54% after 450 min.

It is observed that the TOF value over each of the as-prepared catalysts increased with a rise in reaction temperature. Under the same temperature, in case of HCHO oxidation, the TOF values over the humid gas were much higher than that over the dry gas, with the "RH = 90%" giving the highest TOF values. However in case of CO oxidation, the TOF values over the dry gas were much higher than that over the humid gas.

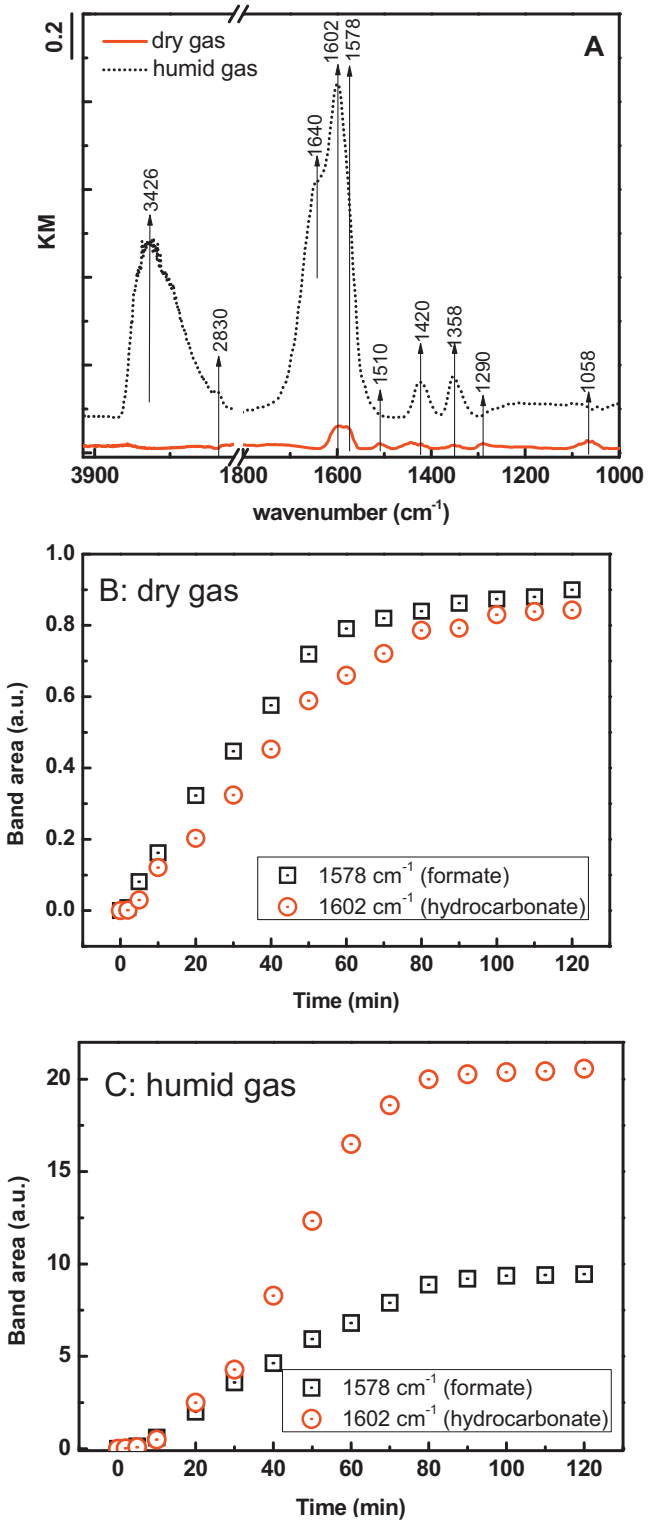

Fig. 3. (A) DRIFT spectra of HCHO adsorption on $Mn_{0.75}Co_{2.25}O_4$ (80 ppm HCHO/21% O_2/H_2O (RH = 0 or 50%)/N_2 balance, GHSV = 60,000 h^{-1}). Intensity of 1578 and 1602 cm^{-1} band areas as a function of the time on stream for (B) 80 ppm HCHO/21% O_2/N_2 balance, and (C) 80 ppm HCHO/21% O_2/H_2O (RH = 50%)/N_2 balance.

3.2. DRIFTS/TPO study of the effect of water on HCHO oxidation

3.2.1. Formation of reaction intermediates

Fig. 3A exhibits in situ DRIFT spectra of $Mn_{0.75}Co_{2.25}O_4$ catalyst after HCHO adsorption in dry and humid (RH = 50%) air streams at room temperature for 120 min. The characteristic bands are

Table 2
Adsorbed species formed during exposure of $Mn_{0.75}Co_{2.25}O_4$ catalyst to HCHO at RT.

Species	Wave number (cm^{-1})
H_2O	3409, 1640
HCHO	1787
Formate	1578, 1358, 2800–2830
Hydrocarbonate	1602, 1420
Bidentate carbonate	1290, 1058
Monodentate carbonate	1510, 1340

reported in Table 2. Upon exposure to a dry air stream (80 ppm HCHO/21% O_2/N_2 balance) peaks ascribed to formate species (2800, 1578 and 1358 cm^{-1}) [36,37], hydrocarbonates (1602 and 1420 cm^{-1}) [38,39], and carbonate species (1510, 1290, 1058 and 1340 cm^{-1}) [38–40] appeared. These results are indicative of the partial oxidation of HCHO to form formate species, which could further combine with surface oxygen to form hydrocarbonate and carbonate species. In a humid air stream, bands associated with adsorbed water (3426 and 1640 cm^{-1}) were observed [37]. Furthermore, bands ascribable to formate species and hydrocarbonates were also detected. However, carbonate species were not observed, unlike the result obtained with the dry air stream.

To check the relative concentrations of the formate and hydrocarbonate intermediates in dry air and humid air, the variation in the measured integrated intensities of the formate (1578 cm^{-1}) and hydrocarbonate (1602 cm^{-1}) bands was monitored as a function of time, as shown in Fig. 3B and C. Upon exposure to HCHO in flowing dry air, the intensities of the bands due to formate and hydrocarbonates species increased rapidly with exposure time and reached a near constant value after 80 min; as shown in Table 3, the 1602/1578 cm^{-1} peak area ratio of was calculated to be 0.93 after adsorption for 120 min. In comparison, in flowing humid air, the area of the hydrocarbonate band at 1602 cm^{-1} was much higher than that of the formate band at 1578 cm^{-1}, the final 1602/1578 cm^{-1} peak area ratio being 2.25. This comparison clearly demonstrates that the presence of H_2O in the gas stream accelerated the further oxidation of the formates into hydrocarbonate.

TPO experiments were conducted after the sample was exposed to flowing HCHO with and without H_2O in the feed, the results being shown in Fig. 4A and B, respectively. By means of curve-fitting, the distribution of CO_2 species was estimated, as shown in Table 3. For the experiment using dry air, shown in Fig. 4A, CO_2 evolution maxima were observed at 145, 165 and 285 °C. In order to identify the origin of the peaks at 145 and 165 °C, TPO was conducted over a CoMn catalyst prepared by a citric acid method (denoted hereinafter as CoMn-CA) as reported in our previous work [29] (Fig. 3S). We have previously shown by in situ DRIFTS that formate was the only reaction intermediate formed during HCHO partial oxidation at R.T. over the CoMn–CA catalyst. TPO results for the CoMn–CA showed that the main peak for CO_2 evolution occurred at 165 °C, corresponding to oxidation of the formate species on the catalyst surface. Hence, it is reasonable to assign the peaks for CO_2 evolution at 145 and 165 °C to the respective decomposition of hydrocarbonate species and the oxidation of formate species on the $Mn_{0.75}Co_{2.25}O_4$ catalyst surface. From this it follows that the peak at 285 °C was due to the decomposition of monodentate and bidentate carbonate species, which were detected by in situ DRIFTS as shown in Fig. 3A.

For the experiment using humid gas, results were somewhat different as shown in Fig. 4B. Based on the results of curve fitting a comparatively larger CO_2 evolution peak appeared at 145 °C, together with a shoulder 165 °C, indicating that relatively more hydrocarbonate species than formate species were formed. Moreover, the peak for CO_2 evolution arising from the decomposition of carbonate species shifted to a lower temperature (265 °C) and the peak area decreased significantly. These results suggest that

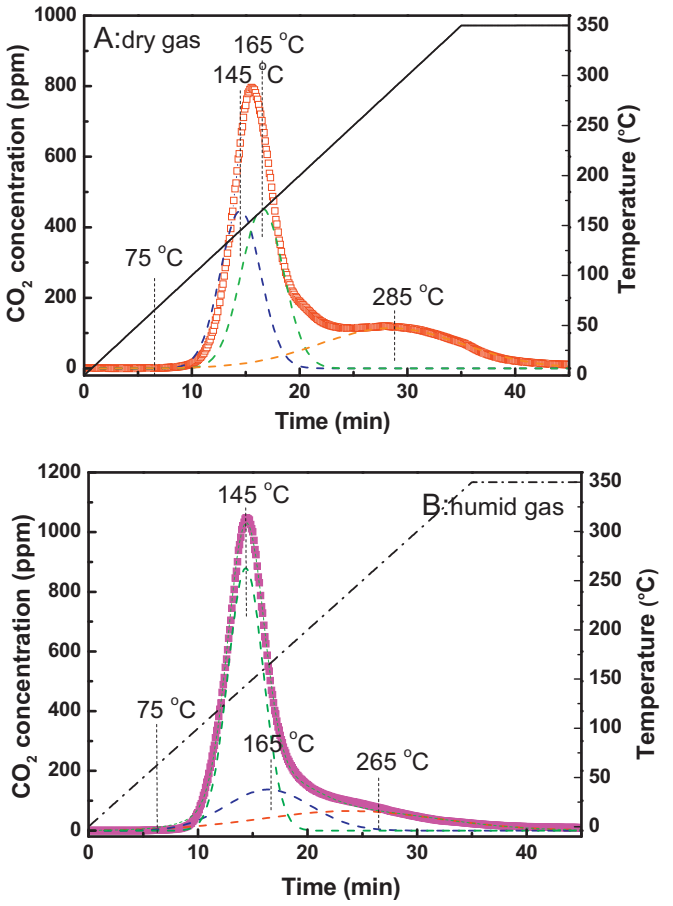

Fig. 4. TPO profiles after the adsorption of (A) 80 ppm HCHO/21% O_2/N_2 balance and (B) 80 ppm HCHO/21% O_2/H_2O (RH = 50%)/N_2 balance on the $Mn_{0.75}Co_{2.25}O_4$ catalyst (TPO conditions: flow rate of 21% O_2/N_2 = 100 ml/min, heating rate = 10 °C/min).

there was less accumulation of surface carbonate compared to the experiment using dry gas and that the carbonate was more easily decomposed. The 145/165 °C peak area ratios were calculated for the experiments using dry and humid feeds as shown in Table 3, the respective values being 0.94 and 2.68. From this it follows that relatively more hydrocarbonate species were generated in the humid gas, which is in good agreement with the results of the DRIFTs analysis.

3.2.2. Consumption of reaction intermediates

Shown in Fig. 5 are DRIFT spectra recorded under dry and humid air streams(containing 21% O_2/H_2O (RH = 0 or 50%)/N_2 balance) at elevated temperatures after the catalyst was first exposed to a flow of 80 ppm HCHO/21% O_2/N_2 balance at 25 °C for 120 min. In all cases spectra were obtained after steady state had been reached. In the case of the dry air feed (Fig. 5A), no obvious decrease in hydrocarbonate or formate band intensities was observed at 50 or 60 °C. However, upon heating to 75 °C, the intensities of the bands at 1602 and 1420 cm^{-1} due to the hydrocarbonates, and at 1578 and 1358 cm^{-1} due to the formates decreased sharply. Complete oxidation of these species occurred at 90 °C.

In contrast, for the humid air feed (Fig. 5B), upon on standing at 50 °C for 40 min, bands at 3426 and 1640 cm^{-1} ascribable to adsorbed water were observed, while the band intensities at 1602 cm^{-1} due to hydrocarbonates and 1578 cm^{-1} due to the formates began to decrease at 50 °C. Upon heating to 60 °C, the characteristic peaks due to hydrocarbonates disappeared, while only a very weak peak due to the formates could be observed. Upon heating to 75 °C, only bands associated with adsorbed H_2O could be

Table 3
Comparison of hydrocarbonate/formate ratios calculated from TPO and DRIFTs results.

	Integral peak area from TPO (a.u.)				Integral peak area from DRIFTs (a.u.)[a]		
	$X_{145\,^\circ C}$	$X_{165\,^\circ C}$	$X_{285\,^\circ C}$	$X_{145\,^\circ C}/X_{165\,^\circ C}$	$X_{1578\,cm^{-1}}$	$X_{1602\,cm^{-1}}$	$X_{1602\,cm^{-1}}/X_{1578\,cm^{-1}}$
Dry gas	2090	2215	1890	0.94	0.84	0.78	0.93
Humid gas	3560	1330	1338	2.68	8.88	20.01	2.25

[a] Integral peak area from DRIFTs after adsorption for 120 min.

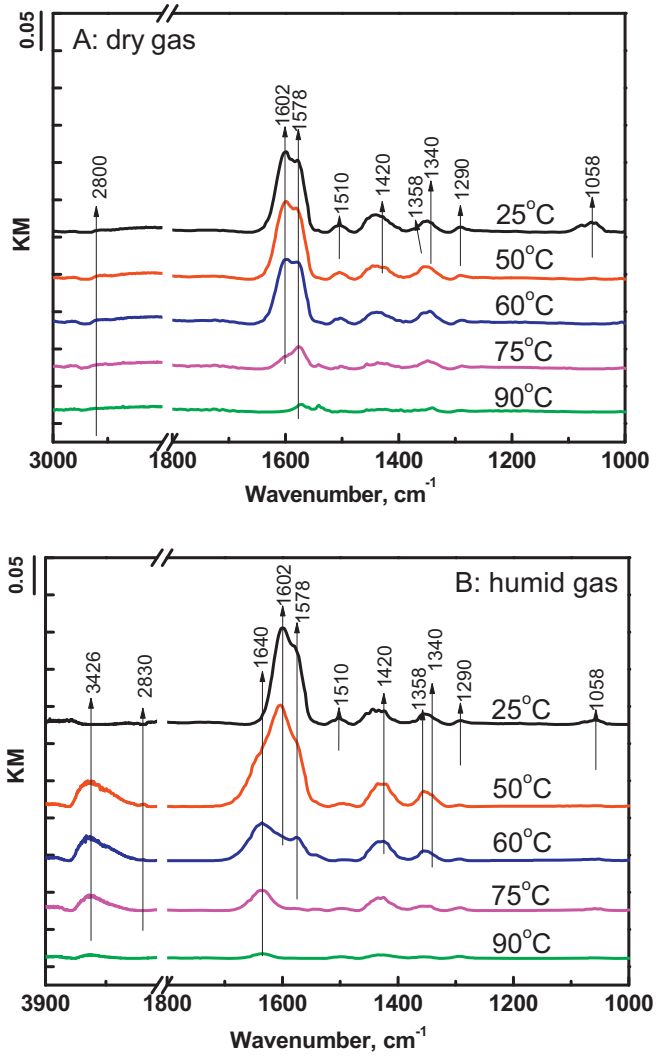

Fig. 5. DRIFT spectra collected on $Mn_{0.75}Co_{2.25}O_4$ catalyst upon temperature increase in (A) 21% O_2/N_2 balance and (B) 21% O_2/H_2O (RH = 50%)/N_2 balance streams.

observed. Noteworthy was the fact that the temperature for oxidation of the intermediates significantly decreased in humid air, implying that the presence of water in the gas stream accelerated the oxidation of the formates and hydrocarbonates. It was also found that the temperatures for complete oxidation of these intermediates coincided with those for complete conversion of HCHO into CO_2 and H_2O (Fig. 2S).

To investigate the residual species on the catalyst surface after the extended HCHO oxidation tests described in Section 3.1, TPO experiments were conducted on the used catalysts, the results being shown in Fig. 6. Peaks corresponding to CO_2 evolution were observed in the low and high temperature regions, which can be assigned to the oxidation of surface intermediates and to the decomposition of carbonate species, respectively, based on the results shown in Fig. 4. Compared with the sample used in humid

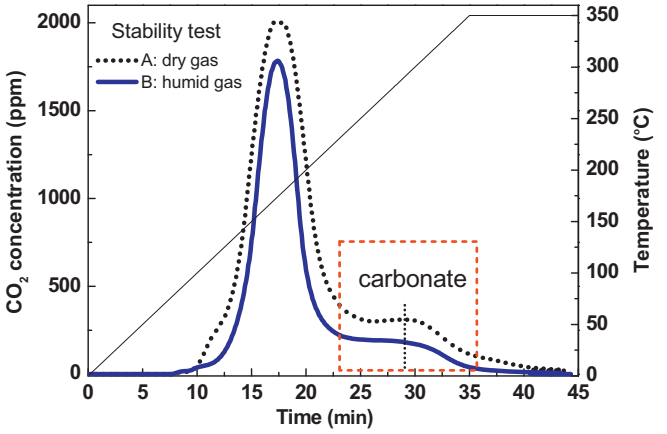

Fig. 6. TPO profiles after HCHO oxidation stability test performed on $Mn_{0.75}Co_{2.25}O_4$ catalyst (TPO conditions: flow rate of 21% O_2/N_2 = 100 ml/min, heating rate = 10 °C/min; stability test conditions: (A) 80 ppm HCHO/21% O_2/N_2 balance and (B) 80 ppm HCHO/21% O_2/H_2O (RH = 50%)/N_2 balance, reaction time = 1800 min, GHSV = 60,000 h^{-1}, reaction temperature: 70 °C).

air, a larger CO_2 peak ascribed to the decomposition of carbonate species was observed for the sample used in dry air. This suggests that a higher concentration of carbonate species accumulated on catalyst surface during the reaction in dry air, which may be responsible for the gradual deactivation of the catalyst evident in Fig. 1C. Upon thermal treatment at 350 °C, the activity of the regenerated catalyst for HCHO oxidation matched that of the fresh catalyst (Fig. 1C). Hence, the loss in activity during HCHO oxidation can be ascribed to the accumulation of carbonate species on the surface of the $Mn_{0.75}Co_{2.25}O_4$ catalyst.

3.3. Study on the negative effect of moisture on activity/positive effect on stability for CO oxidation

To investigate the variation in gas phase CO, CO_2 and H_2O concentration in the reactor effluent with TOS (at room temperature) MS–IRAS experiments were performed, the results being presented in Fig. 7. In dry gas, as shown in Fig. 7A, the CO concentration at the reactor outlet decreased to ca. 0 ppm immediately, while the CO_2 concentration (Fig. 7B) increased to ca. 500 ppm after 10 min, and then remained unchanged. In contrast, in humid air (RH = 20–70%), the CO concentration immediately decreased to ca. 0 ppm but rapidly increased to 500 ppm after 8–15 min. Fig. 7B indicates that CO consumption was accompanied by CO_2 formation, consistent with the oxidation of CO into CO_2. Fig. 7C shows the variation in H_2O concentration during this period. Clearly, the higher the R.H., the more water was adsorbed on the catalyst, and the faster the catalyst lost its activity, indicating a poisoning effect of water.

Fig. 8A shows DRIFTs spectra obtained following sequential treatment of the $Mn_{0.75}Co_{2.25}O_4$ catalyst with H_2O and CO at 20 °C. The characteristic bands are reported in Table 4. The sample was first treated with H_2O/N_2 for 60 min, resulting in the observation of bands due to H_2O at 3420, 1649, 1433, and 1340 cm^{-1}). The feed stream was then switched to 500 ppm CO/20% O_2/N_2, resulting in

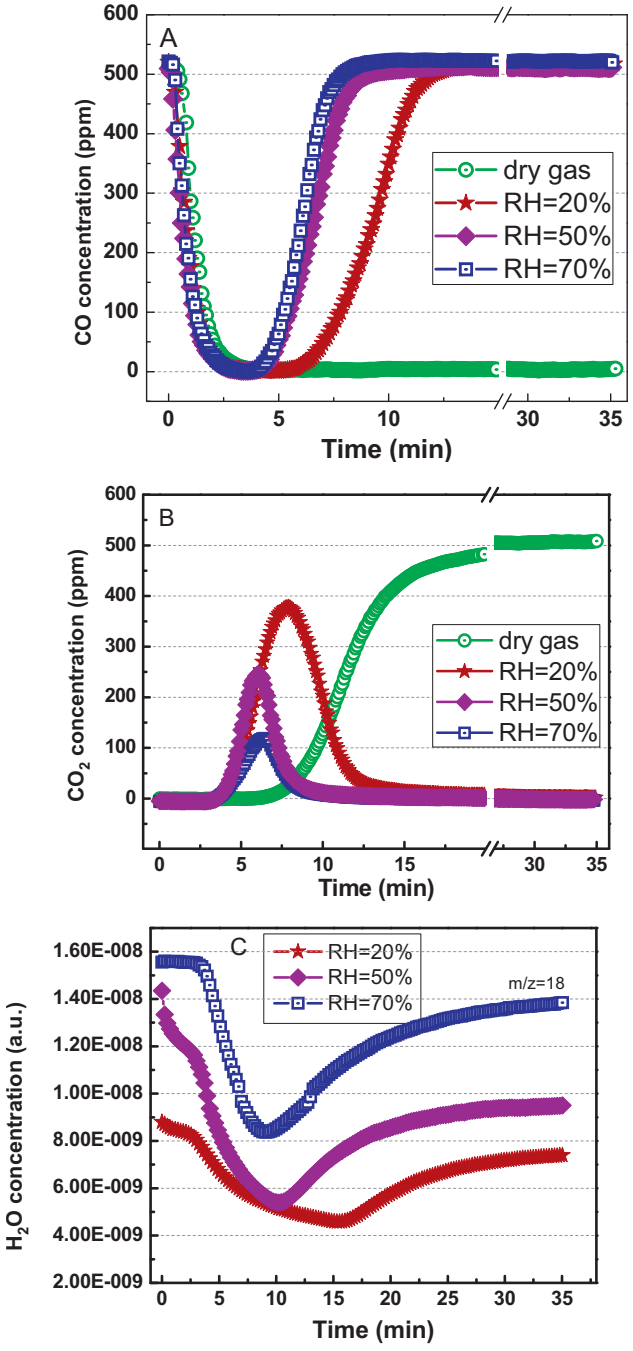

Fig. 7. CO (A), CO_2 (B), and H_2O (C) concentrations in reactor effluent versus time on stream during CO oxidation over $Mn_{0.75}Co_{2.25}O_4$; 500 ppm CO/20% O_2/H_2O (RH = 0–70%)/N_2 balance as feed, GHSV = 60,000 h^{-1}, reaction temperature = 20 °C.

Table 4
Adsorbed species formed during exposure of $Mn_{0.75}Co_{2.25}O_4$ catalyst to CO at RT.

Species	Wave number (cm^{-1})
H_2O	3420, 1649, 1433, 1340
CO	2142
CO_2	2340, 2360
Bidentate carbonate	1540, 1330, 1280, 1036
Monodentate carbonate	1350, 1375, 1390
Polymeric carbonate and formates	1600–1400

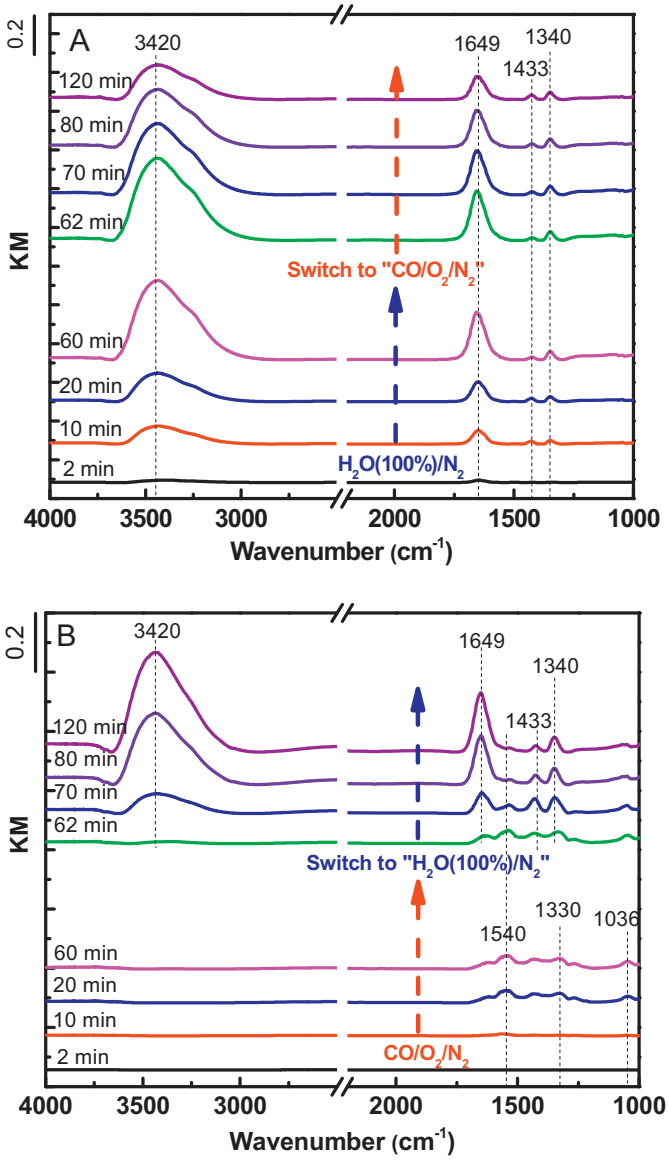

Fig. 8. DRIFT spectra of CO oxidation over $Mn_{0.75}Co_{2.25}O_4$ versus time on stream at 20 °C. (A) First H_2O (RH = 100%)/N_2 balance as feed for 60 min, then 500 ppm CO/20% O_2/N_2 balance. (B) First 500 ppm CO/20% O_2/N_2 balance as feed for 60 min, then H_2O (RH = 100%)/N_2 balance.

a decrease in intensity of the bands due to adsorbed H_2O. Unlike the case when CO was directly adsorbed on the catalyst (shown in Fig. 4S), bands due to carbonates were not observed during the sequential treatment with H_2O and CO, which may be due to water molecules strongly adsorbing on the catalyst, thus blocking CO adsorption.

DRIFTs spectra obtained following sequential treatment of the $Mn_{0.75}Co_{2.25}O_4$ catalyst with CO and then H_2O at 20 °C are presented in Fig. 8B. The sample was first treated with 500 ppm CO/20% O_2/N_2 for 60 min, resulting in the observation of bands due to bidentate carbonate species (bands at 1540, 1330, and 1036 cm^{-1}). The feed was then switched to H_2O/N_2, which led to the progressive disappearance of the carbonate species. Meanwhile, bands at 3420, 1649, 1433, and 1340 cm^{-1} due to H_2O gradually increased in intensity with time on stream. Therefore, it was clear that H_2O was strongly absorbed on the catalyst, to the extent that carbonate was replaced.

DRIFTS spectra obtained following sequential treatment of the $Mn_{0.75}Co_{2.25}O_4$ catalyst with H_2O and CO at 100 °C are presented in

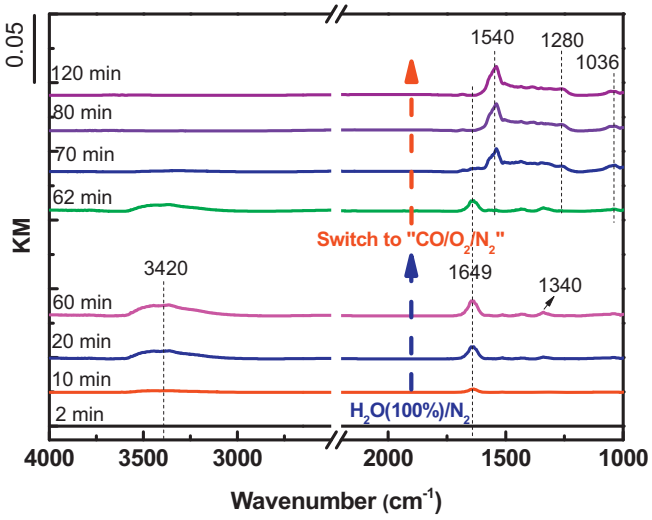

Fig. 9. DRIFT spectra of CO oxidation over $Mn_{0.75}Co_{2.25}O_4$ versus time on stream at 100 °C; feed: first H_2O (RH = 100%)/N_2 balance for 60 min, then 500 ppm CO/20% O_2/N_2 balance.

Fig. 9. Due to the higher temperature, the adsorption of water at the active sites was greatly diminished compared to the experiment at 20 °C. Exposing the sample pre-treated with H_2O to 500 ppm $CO/O_2/N_2$ resulted in the fast disappearance of the bands at 3420, 1649, 1433, and 1340 cm^{-1} due to H_2O, while bands at 1540, 1280, and 1036 cm^{-1} which have been assigned to bidentate carbonate species gradually increased in intensity with time on stream.

TPO experiments were conducted on the catalyst after the long duration CO oxidation test, the results being shown in Fig. 10. For the catalyst used in the humid air feed, CO_2 evolution was negligible. However, the TPO profile for the catalyst used with the dry air feed was very different. Specifically, two peaks were observed for CO_2 formation, corresponding to temperatures of 156 °C and at 270 °C, which can be assigned to the decomposition of formates and monodentate species, respectively. This implies that the catalyst surface was in large part covered by carbonate compounds which were stable at low temperatures. These species were the cause of the gradual catalyst deactivation.

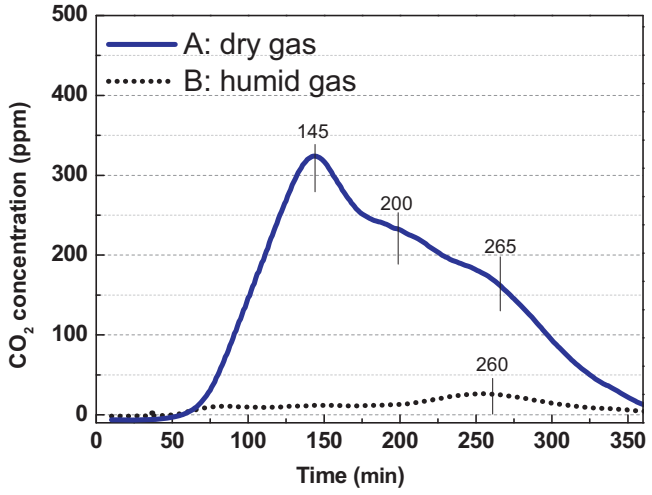

Fig. 10. TPO profiles after CO oxidation stability test performed using $Mn_{0.75}Co_{2.25}O_4$ catalyst (TPO conditions: flow rate of 20% O_2/N_2 = 100 ml/min, heating rate = 10 °C/min; stability test conditions: (A) 500 ppm CO/20% O_2/N_2 balance and (B) 500 ppm CO/20% O_2/H_2O (RH = 50%)/N_2 balance, reaction time = 450 min, GHSV = 240,000 h^{-1}, reaction temperature = 90 °C).

4. Discussion

4.1. Effect of H_2O on complete oxidation of HCHO

The promoting effect of H_2O on complete oxidation of HCHO has been reported for several noble metal catalysts, such as Pt/Fe_2O_3, Au/CeO_2 and $Ag–MnO_x–CeO_2$, and over metal oxides such as manganese oxides. An et al. [20] found that the activity of Pt/Fe_2O_3 could be considerably improved by addition of 3% water vapor into the reactant stream, such that the conversion of HCHO reached 100% at room temperature. Moreover, in previous work [21] we found that although 100% conversion could be achieved in both dry and wet air over Au/CeO_2, water had a positive effect both on the formation and consumption of the formate reaction intermediates, leading to enhanced HCHO removal efficiency in wet air. Furthermore, Zhao et al. [22] reported the enhanced effect of water vapor on catalytic oxidation of formaldehyde with ozone to CO_2 over MnO_x catalysts at room temperature. It was found that the selectivity to CO_2 was greatly enhanced in humid air, whereas in dry air HCHO was mostly oxidized to CO. Herein, $Mn_{0.75}Co_{2.25}O_4$ catalyst prepared by co-precipitation was investigated as a catalyst for HCHO oxidation. The activity of $Mn_{0.75}Co_{2.25}O_4$ was promoted in humid air and the conversion was more stable than in dry air. This is significant for practical use, given that the presence of water is inevitable in air.

The formation and consumption of reaction intermediates was investigated using in situ DRIFTS and TPO. In the case of dry air streams, the adsorption of HCHO is the first step prior to oxidation to formaldehyde. It is apparent that HCHO could be rapidly oxidized into formate species [37,41] in both dry and humid air over the $Mn_{0.75}Co_{2.25}O_4$ catalyst (step (1a) below). A second attack of surface active oxygen at the C—H bond of the formates generates hydrocarbonate species (step (1b)) [41,42]. Deactivation during HCHO oxidation may occur by the transformation of the hydrocarbonates into carbonates at the active site by dehydration as shown in Eq. (1c) [3,43,44] (the reacting OH groups are already present on the surface which is known that the OH groups on a catalyst surface are to some extent mobile). In humid air (pathway B), it is clear that the presence of H_2O in the feed exerts a promoting effect on the rate of hydrocarbonate formation, which has been reported elsewhere [3,21]. It is postulated that introduction of water into the feed gas generates hydroxyl groups ($M–O–M + H_2O \rightarrow 2M–OH$) on the catalyst surface [3,44,45]; in this way water can facilitate the activation of O_2 molecules, thereby participating in the oxidation of formates to hydrocarbonates (step (2)). The ability of water to reverse carbonate formation (the reverse reaction of step (1c)) under humid conditions explains why its presence can prevent the catalyst from deactivating [3,45]. We consider that water plays two roles in the formation of the intermediates: one is the generation of surface $[OH]_s$, which facilitates the oxidation of $[HCOO^-]_s$ into $[HCO_3^-]_s$; the other is suppression of the formation of inactive carbonate species.

$$HCHO\ (ad) + [O]_s \rightarrow [HCOO^-]_s + [H^+]_s \quad (1a)$$

$$[HCOO^-]_s + [O]_s \rightarrow [HCO_3^-]_s \quad (1b)$$

$$[HCO_3^-]_s + [OH]_s \leftrightarrow [CO_3^{2-}]_s + H_2O \quad (1c)$$

$$[HCOO^-]_s + [OH]_s \rightarrow [HCO_3^-]_s + [H^+]_s \quad (2)$$

The consumption of the reaction intermediates at elevated temperature was also studied. As proved by the DRIFTS and TPO results, hydrocarbonate species can be directly decomposed into CO_2 and OH (step (3a)) at elevated temperatures [3]. The formates react with surface [O] and $[H^+]$ to produce CO_2 (g) and H_2O [21] (Eq. (3b)). In humid air, hydrocarbonate species may combine with H^+ to generate CO_2 (g) and H_2O very quickly (step (4a)) [41], which accelerates the decomposition rate of the hydrocarbonate species. Meanwhile,

surface hydroxyl groups react with the formates to generate CO_2 (g) and H_2O (step (4b)), which has been shown to be another pathway for formate oxidation [6].

$$[HCO_3^-]_s \rightarrow CO_2(g) + [OH]_s \quad (3a)$$

$$[HCOO^-]_s + [O]_s + [H^+]_s \rightarrow CO_2(g) + H_2O \quad (3b)$$

$$[HCO_3^-]_s + [H^+]_s \xrightarrow[\Delta]{} CO_2\ (g) + H_2O \quad (4a)$$

$$[HCOO^-]_s + [OH] \xrightarrow[\Delta]{} CO_2\ (g) + H_2O \quad (4b)$$

In summary, water was found to play key role in the oxidation of HCHO over the $Mn_{0.75}Co_{2.25}O_4$ catalyst. It is postulated that the introduction of water provides a second role for complete oxidation of HCHO, by promoting both the formation and the consumption of reaction intermediates, as well as the decomposition of surface carbonates.

4.2. Effect of H_2O on complete oxidation of CO

It is generally accepted that deactivation resulting from the presence of water is the main obstacle currently limiting the application of metal oxides catalyst to CO oxidation at low temperatures. Co_3O_4 displays extraordinarily high activity for CO oxidation at very low temperatures (ca. −77 °C). However, in the presence of trace amounts of water, its activity is dramatically reduced [14]. Zhang et al. [46] studied the effect of H_2O and CO_2 in the reactant stream on the performance of a Mn–Co–O catalyst in the preferential oxidation (PROX) of CO, and found that the inhibiting effect of H_2O is stronger than that of CO_2, which may be related to blockage of the active site by H_2O at ≤100 °C. In the present study, possible deactivation pathways of $Mn_xCo_{3-x}O_4$ with regard to water were investigated and the roles of water in affecting the catalyst activity and stability were clarified.

Based on the results of DRIFTS, MS–IRAS and TPO described above, reaction pathways are proposed for oxidation of CO over $Mn_{0.75}Co_{2.25}O_4$ catalyst in dry and humid air streams. Step (5) represents the reaction pathway in the absence of H_2O as discussed before [3]. Briefly, CO is adsorbed and activated on the catalyst, while O_2 is captured and activated by the oxygen vacancy in $Mn_{0.75}Co_{2.25}O_4$. Then, $[CO]_s$ and $[O]_s$ were formed $[COO]_s$ intermediate species, and the $[COO]_s$ intermediate needed time to accumulate, when the $[COO]_s$ intermediate reached a certain concentration, CO_2 is then formed (step (5a)), which can explain the phenomenon why the peak of CO and CO_2 concentration appeared at different time in Fig. 7. However, in dry conditions, the catalyst surface are gradually covered by the carbonate species accumulated during the reaction (step (5b)), so that the activity steadily decreases.

$$[CO]_s + [O]_s \rightarrow [COO]_s \rightarrow CO_2(g) \quad (5a)$$

$$[COO]_s + [O]_s \rightarrow [CO_3^{2-}]_s \quad (5b)$$

When H_2O is present in the feed, the active sites are gradually blocked, via three possible processes: (i) H_2O dissociative adsorption on the [O] vacancies; (ii) H_2O dissociative adsorption on metal cations (Co or Mn); and (iii) molecular adsorption of H_2O on metal cations (Co or Mn). In principle, any of these processes may hinder the adsorption of CO and oxygen. Another possible cause of deactivation of $Mn_{0.75}Co_{2.25}O_4$ can be ascribed to the conversion of surface lattice O to OH groups, it having been shown that surface OH groups are inert with respect to CO oxidation at low temperature [47]. However, sufficient drying of the catalyst ensures the availability of active sites for the adsorption of carbon monoxide (Fig. 9), the increased CO conversion obtained with increase of temperature from 90 to 100 °C under humid conditions being in agreement with this hypothesis [48]. Notably, the removal of carbonates, corresponding to the reverse of step (1c), which results in regeneration of the catalyst, requires the involvement of water. The ability of water to reverse carbonate formation also explains why its presence in the reaction mixture can prevent catalyst deactivation during extended operation.

In summary, water has two possible roles during CO oxidation. First, it may block the active sites on the surface, hindering CO and O_2 adsorption. The second possible role of water is assisting in the decomposition of carbonates, which leads to improved stability for CO oxidation in humid conditions.

An obvious question is why the effect of the water on HCHO and CO oxidation activity is so different for the same metal oxide surfaces. We believe that water solubility may be a key factor. Sidheswaran et al. [28] found a slight decrease in formaldehyde removal efficiency at high ambient humidity conditions, which can be attributed to the competitive adsorption of water on the surface of the catalyst. However, when the humidity in the system was decreased back to lower RH, the removal efficiency of formaldehyde increased, showing the ability of the catalyst to regenerate at lower humidity. Sidheswaran et al. [28] attributed the phenomenon to that formaldehyde is soluble in water and hence can be trapped reversibly in the sorbed aqueous layer, leading to consistent removal of formaldehyde with minimal effect on catalyst performance upon changes in the relative humidity. However, CO is water-insoluble; hence, CO cannot penetrate the sorbed aqueous layer, thereby hindering its adsorption. Moreover, any surface OH groups formed are inactive in CO oxidation compared to lattice O.

5. Conclusions

The effect of moisture on the activity and stability of HCHO and CO oxidation over $Mn_{0.75}Co_{2.25}O_4$ catalyst is reported for the first time. The results of in situ DRIFTS measurements and TPO experiments showed that, in the case of HCHO oxidation, water (RH = 0–90%) plays two roles in HCHO oxidation, benefitting both the formation and the consumption of reaction intermediates, as well as the removal of carbonates; this results in enhanced catalyst activity and stability in humid air. In the case of CO oxidation, it was found that H_2O may block the active sites on the surface and thereby hinder CO_2 production. However, the presence of water was also beneficial for the decomposition of carbonates, which prolonged the catalyst lifetime in humid air.

Acknowledgments

The work was supported by the National Natural Science Foundation of China (Nos. 21073024 and 21373037).

Appendix A. Supplementary data

Supplementary data associated with this article can be found, in the online version, at http://dx.doi.org/10.1016/j.apcatb.2014.06.011.

References

[1] Y. Sekine, Atmos. Environ. 36 (2002) 5543–5547.
[2] Y. Sekine, A. Nishimura, Atmos. Environ. 35 (2001) 2001–2007.
[3] M. Date, M. Okumura, S. Tsubota, M. Haruta, Angew. Chem. Int. Ed. Engl. 43 (2004) 2129–2132.
[4] A.S. Hashmi, G.J. Hutchings, Angew. Chem. Int. Ed. Engl. 45 (2006) 7896–7936.
[5] M. Mavrikakis, P. Stoltze, J.K. Nørskov, Catal. Lett. 64 (2000) 101–106.
[6] S. Ebbesen, B. Mojet, L. Lefferts, J. Catal. 246 (2007) 66–73.
[7] H. Kung, M.C. Kung, C.K. Costello, J. Catal. 216 (2003) 425–432.
[8] S.D. Ebbesen, B.L. Mojet, L. Lefferts, PCCP 11 (2009) 641–649.
[9] Q. Sun, K. Reuter, M. Scheffler, Phys. Rev. B: Condens. Matter 67 (2003).
[10] J. Bergeld, B. Kasemo, D.V. Chakarov, Surf. Sci. 495 (2001) 815–820.

[11] F. Liang, H. Zhu, Z. Qin, H. Wang, G. Wang, J. Wang, Catal. Lett. 126 (2008) 353–360.
[12] J. Jansson, J. Catal. 194 (2000) 55–60.
[13] Y. Yu, T. Takei, H. Ohashi, H. He, X. Zhang, M. Haruta, J. Catal. 267 (2009) 121–128.
[14] X. Xie, Y. Li, Z.Q. Liu, M. Haruta, W. Shen, Nature 458 (2009) 746–749.
[15] H. Zou, X. Dong, W. Lin, Appl. Surf. Sci. 253 (2006) 2893–2898.
[16] K. Sirichaiprasert, A. Luengnaruemitchai, S. Pongstabodee, Int. J. Hydrogen Energy 32 (2007) 915–926.
[17] F. Grillo, Appl. Catal., B: Environ. 48 (2004) 267–274.
[18] J. Wonpark, J. Hyeokjeong, W. Yoon, C. Kim, D. Lee, Y. Park, Y. Rhee, Int. J. Hydrogen Energy 30 (2005) 209–220.
[19] W. Guiying, Z. Wenxiang, C. Yunchen, L. Honglei, J. Dazhen, W. Tonghao, Chin. J. Catal. 22 (2001) 408–410.
[20] N. An, Q. Yu, G. Liu, S. Li, M. Jia, W. Zhang, J. Hazard. Mater. 186 (2011) 1392–1397.
[21] B.-B. Chen, C. Shi, M. Crocker, Y. Wang, A.-M. Zhu, Appl. Catal., B: Environ. 132-133 (2013) 245–255.
[22] D.Z. Zhao, C. Shi, X.S. Li, A.M. Zhu, B.W. Jang, J. Hazard. Mater. 239–240 (2012) 362–369.
[23] C. Shi, B.-b. Chen, X.-s. Li, M. Crocker, Y. Wang, A.-m. Zhu, Chem. Eng. J. 200–202 (2012) 729–737.
[24] H. Huang, X. Ye, H. Huang, L. Zhang, D.Y.C. Leung, Chem. Eng. J. 230 (2013) 73–79.
[25] Z. Wang, J. Pei, J. Zhang, Build. Environ. 65 (2013) 49–57.
[26] D.-Z. Zhao, X.-S. Li, C. Shi, H.-Y. Fan, A.-M. Zhu, Chem. Eng. Sci. 66 (2011) 3922–3929.
[27] X. Tang, Y. Li, X. Huang, Y. Xu, H. Zhu, J. Wang, W. Shen, Appl. Catal., B: Environ. 62 (2006) 265–273.
[28] M.a. Sidheswaran, H. Destaillats, D.P. Sullivan, J. Larsen, W.J. Fisk, Appl. Catal., B: Environ. 107 (2011) 34–41.
[29] C. Shi, Y. Wang, A. Zhu, B. Chen, C. Au, Catal. Commun. 28 (2012) 18–22.
[30] Y. Wang, A. Zhu, B. Chen, M. Crocker, C. Shi, Catal. Commun. 36 (2013) 52–57.
[31] M. Alifanti, M. Florea, S. Somacescu, V. Parvulescu, Appl. Catal., B: Environ. 60 (2005) 33–39.
[32] C.T. Wong, A.Z. Abdullah, S. Bhatia, J. Hazard. Mater. 157 (2008) 480–489.
[33] Y.X. Liu, H.X. Dai, Y.C. Du, J.G. Deng, L. Zhang, Z.X. Zhao, C.T. Au, J. Catal. 287 (2012) 149–160.
[34] X. Yang, Y. Shen, L. Bao, H. Zhu, Z. Yuan, React. Kinet. Catal. Lett. 93 (2008) 19–25.
[35] J. Quiroz Torres, S. Royer, J.-P. Bellat, J.-M. Giraudon, J.-F. Lamonier, ChemSusChem 6 (2013) 578–592.
[36] Y. He, H. Ji, Chin. J. Catal. 31 (2010) 171–175.
[37] C. Zhang, F. Liu, Y. Zhai, H. Ariga, N. Yi, Y. Liu, K. Asakura, M. Flytzani-Stephanopoulos, H. He, Angew. Chem. Int. Ed. Engl. 51 (2012) 9628–9632.
[38] C. Binet, M. Daturi, J.C. Lavalley, Catal. Today 50 (1999) 207–225.
[39] C. Laberty, C. Marquez-Alvarez, C. Drouet, P. Alphonse, C. Mirodatos, J. Catal. 198 (2001) 266–276.
[40] B. Liu, C. Li, Y. Zhang, Y. Liu, W. Hu, Q. Wang, L. Han, J. Zhang, Appl. Catal., B: Environ. 111-112 (2012) 467–475.
[41] C. Ma, D. Wang, W. Xue, B. Dou, H. Wang, Z. Hao, Environ. Sci. Technol. 45 (2011) 3628–3634.
[42] D.C. Mc, J.H. Thomas, R.G. Norrish, Nature 162 (1948) 367.
[43] C.K. Costello, J.H. Yang, H.Y. Law, Y. Wang, J.N. Lin, L.D. Marks, M.C. Kung, H.H. Kung, Appl. Catal., A: Gen. 243 (2003) 15–24.
[44] S. Royer, D. Duprez, ChemCatChem 3 (2011) 24–65.
[45] Z. Zheng, J. Teo, X. Chen, H. Liu, Y. Yuan, E.R. Waclawik, Z. Zhong, H. Zhu, Chem.—Eur. J. 16 (2010) 1202–1211.
[46] Q. Zhang, X. Liu, W. Fan, Y. Wang, Appl. Catal., B: Environ. 102 (2011) 207–214.
[47] H.F. Wang, R. Kavanagh, Y.L. Guo, Y. Guo, G.Z. Lu, P. Hu, Angew. Chem. Int. Ed. Engl. 51 (2012) 6657–6661.
[48] D.A.H. Cunningham, T. Kobayashi, N. Kamijo, M. Haruta, Catal. Lett. 25 (1994) 257–264.